

# **Maternal behavioural thermoregulation facilitated evolutionary transitions from egg laying to live birth**

Amanda K. Pettersen<sup>1\*</sup>, Nathalie Feiner<sup>1</sup>, Daniel W.A. Noble<sup>2</sup>, Geoffrey M. While<sup>3</sup>, Tobias Uller<sup>1#</sup> & Charlie K. Cornwallis<sup>1#</sup>

1. Department of Biology, Lund University, Lund, 22 362, Sweden
2. Division of Ecology and Evolution, Research School of Biology, The Australian National University, Canberra, 2600, Australia
3. School of Natural Sciences, University of Tasmania, Hobart, 7005, Australia

\*Corresponding author: [amanda.pettersen@sydney.edu.au](mailto:amanda.pettersen@sydney.edu.au)

#Joint senior author

**Keywords:** Viviparity, Oviparity, Thermal plasticity, Behavioural plasticity, Reproductive mode, Squamates, Lizards, Snakes

1 **Abstract**

2 Live birth is a key innovation that has evolved from egg laying ancestors over 100 times in  
3 reptiles. However, egg-laying lizards and snakes often have preferred body temperatures that  
4 are lethal to developing embryos and should prevent egg retention: how has viviparity  
5 repeatedly evolved in the face of this pervasive mismatch? We resolve this paradox by  
6 conducting phylogenetic analyses of adult and embryo thermal preferences across 224  
7 species. Thermal mismatches between mothers and offspring are widespread but resolved by  
8 gravid females down-regulating their body temperature towards the thermal optimum of  
9 embryos. Importantly, this thermoregulatory behaviour evolved in ancestral egg-laying  
10 species before the evolution of live birth. Maternal thermoregulatory behaviour therefore  
11 bypasses the constraints imposed by a slowly evolving thermal physiology and is likely to  
12 have been a key requirement for repeated transitions to live birth.

## 13 **Introduction**

14 The evolution of live bearing is an important life-history transition in vertebrates (Doody and  
15 Moore, 2010; Lambert and Wiens, 2013; Shine, 1985). The ecological conditions that favour  
16 the transition from egg laying (oviparity) to live birth (viviparity) are relatively well  
17 understood, especially in reptiles, with particularly strong support for the adaptive value of  
18 viviparity in cool climates (Lambert and Wiens, 2013; Shine, 1995). By retaining embryos  
19 throughout development, mothers can buffer offspring from suboptimal nest temperatures,  
20 thereby ensuring faster development, higher hatching success, and increased offspring  
21 viability (Beuchat, 1988a; Le Henanff et al., 2013; Shine, 1995; Warner and Shine, 2007).

22         Despite the adaptive advantages of viviparity, its initial evolution from oviparous  
23 ancestors would seem unlikely. Embryos and adults of oviparous species are adapted to  
24 different thermal environments, with adult lizards and snakes typically having preferred body  
25 temperatures that exceed the upper lethal limit of embryos. For example, the average nest  
26 temperature of the Iberian emerald lizard, *Lacerta schreiberi*, is 24 °C, rarely exceeding 30  
27 °C, while the preferred body temperature of females is 33 °C (Monasterio et al., 2013). Since  
28 embryos are well adapted to the temperatures typically experienced in the nest, they generally  
29 have limited capacity to develop at temperatures outside this range (Du et al., 2019; Noble et  
30 al., 2018b; Sanger et al., 2018). Prolonged exposure to other temperatures, including those  
31 that are optimal for adults, can result in offspring abnormalities and even death (Andrews et  
32 al., 2000; Braña and Ji, 2000; Noble et al., 2018b; Van Damme et al., 1992). A mismatch  
33 between thermal optima of embryos and females should therefore prevent mothers from  
34 retaining embryos throughout development, inhibiting evolutionary transitions to live birth  
35 (Beuchat, 1988b). Notwithstanding this apparent constraint, live birth has evolved over 100  
36 times in squamate reptiles (Blackburn, 2006, 2015a).

37           How can the repeated evolution of viviparity be reconciled with the widespread  
38 thermal mismatch between embryos and adults in oviparous species? There are two potential  
39 scenarios by which viviparity can evolve in the presence of maternal-embryo thermal  
40 mismatches. First, viviparity may only evolve from oviparous ancestors where there is no  
41 mismatch, that is, where adult body temperature ( $P_{bt}$ ) and embryo thermal optima ( $T_{opt}$ ) are  
42 well aligned. Second, females may behaviourally adjust their body temperature when  
43 pregnant to close the gap between adult and embryo thermal optima, even when substantial  
44 mismatches in thermal preferences exist. Such plasticity may come at a cost to female  
45 performance, but temporarily shifting body temperature while gravid to match the thermal  
46 optima of embryos could eliminate thermal barriers to the evolution of viviparity.

47           Explaining how mismatches between female and offspring thermal optima have been  
48 resolved in viviparous lineages is challenging. Adult and embryo thermal preferences of the  
49 oviparous ancestors of viviparous lineages need to be reconstructed using available data on  
50 extant species, but data on thermal preferences across life stages are difficult to obtain. Often  
51 only some measures (preferred body temperature of oviparous adults, optimal incubation  
52 temperature of embryos, plasticity in female thermoregulation) are available for a subset of  
53 species, leading to patchily distributed data (Figure 1). Recent advances in phylogenetic  
54 methods help to resolve such issues, making it possible to infer ancestral states across  
55 multiple traits where information is non-overlapping across species (e.g., values of some  
56 traits are only available for some species and vice versa) (Hadfield and Nakagawa, 2010;  
57 Nakagawa, 2015). The accuracy of such analyses are, however, reliant on the amount of  
58 variation in traits explained by phylogeny (phylogenetic signal) as this determines the  
59 accuracy with which missing values can be predicted (Molina-Venegas et al., 2018).

60           We collated data on the thermal preferences of adult females (163 species) and  
61 embryos (51 species) of squamate reptiles and combined this with data on their reproductive

62 mode (Pyron and Burbrink, 2014) (Tables S1 & S2). First, we examined the ability of  
63 phylogenetic methods to overcome the patchily distributed data on the thermal biology and  
64 reproductive mode of reptiles. These analyses revealed that phylogenetic models were able to  
65 predict ancestral states with a high degree of accuracy with substantial missing data (Table  
66 S3). Second, we estimated the ancestral states of preferred body temperature of adult females  
67 and embryos to quantify the thermal conflict between mothers and embryos (Table S4-S6).  
68 Third, we tested the prediction that transitions to viviparity have been restricted to oviparous  
69 lineages with a low degree of maternal-embryo mismatch (Table S7-S9). This was assessed  
70 by calculating if viviparity has originated more frequently from oviparous ancestors where  
71 female *Pbt* overlaps with the thermal optima of embryos. Finally, we examined if females  
72 adjust their body temperature when gravid to reduce the mismatch between adult and embryo  
73 thermal optima (52 species), and if so, whether this behaviour evolved prior to the emergence  
74 of viviparity, or afterwards in response to such mismatch (Tables S9-S12).

75

## 76 **Results and Discussion**

### 77 *Ancestral state reconstructions with missing data*

78 There was high phylogenetic signal for all traits (phylogenetic heritability (phylo  $H^2$ ) >0.7),  
79 indicating the potential to infer ancestral values of traits given data limitations (Tables S4-S6  
80 & S10). We explicitly tested if models could accurately predict the state of tips and ancestral  
81 nodes using limited data in two ways. First, we compared estimates of ancestral states for  
82 reproductive mode obtained from an analysis of all data on reproductive mode ( $n_{\text{species}} =$   
83 7831), to estimates from an analysis of only species with thermal data on a pruned phylogeny  
84 ( $n_{\text{species}} = 224$ ). We found that 91% of ancestral nodes were predicted to have the same  
85 reproductive mode. Second, we compared two models, one where all data on reproductive  
86 mode were included ( $n_{\text{species}} = 7831$ ), and one where data were restricted to only species with

87 thermal data ( $n_{\text{species}} = 224$ ), with the remaining tips set as missing values ( $n_{\text{species}} = 7608$ ).  
88 These analyses showed that the data on 224 species could be used to correctly predict the  
89 reproductive modes of the 7608 ‘missing’ species with 70% accuracy (Figure 3. All ancestral  
90 reconstructions are presented in Table S3). These results show that phylogenetic methods  
91 can be used accurately predict extensive amounts of missing data, and more specifically,  
92 species for which there were thermal data provided a general representation of the broader  
93 squamate phylogeny.

94

#### 95 *Wide-spread mismatch in thermal optima of oviparous mothers and their embryos*

96 Across oviparous lizards and snakes, many species displayed significant disparity between  
97 adult female preferred body temperature ( $P_{bt}$ ) and the temperature that maximizes hatching  
98 success ( $T_{opt}$ ) (Multi-response BPMM (MR-BPMM): posterior mode (PM) of difference =  
99 3.43, 95% Credible Interval (CI): -2.26, 10.78,  $pMCMC = 0.08$ . Figure 1 & 2; Table S4). The  
100 female  $P_{bt}$  of oviparous species is on average 5 °C higher than the embryonic  $T_{opt}$  (raw data  
101 mean  $\pm$  SD  $P_{bt}$  103 species:  $32.41 \pm 4.15$  °C;  $T_{opt}$  47 species:  $27.15 \pm 2.12$  °C). Incubation  
102 experiments have shown that such a difference can significantly reduce hatching success,  
103 illustrating that exposure to those thermal conditions throughout development via the  
104 retention of offspring may jeopardise embryo survival (reviewed in (Noble et al., 2018b)).  $P_{bt}$   
105 and  $T_{opt}$  of oviparous species were both estimated to evolve slowly (Figure 1; MR-BPMM:  
106  $P_{bt}$  phylo  $H^2$ : 0.92, CI: 0.82, 0.98.  $T_{opt}$  phylo  $H^2$ : 0.92, CI: 0.68, 0.98. Table S5) and female  
107  $P_{bt}$  and offspring  $T_{opt}$  only showed weak evidence of coevolving (Figure 2; phylogenetic  
108 correlation (MR-BPMM): PM = 0.72, CI: -0.36, 0.97,  $pMCMC = 0.18$ . Table S5), suggesting  
109 that this mismatch may be difficult to resolve.

110

#### 111 *Transitions to live birth occur despite mismatches between females and embryos*

112 We found evidence that preferred body temperature was lower in viviparous, compared with  
113 oviparous, lineages (MR-BPMM: PM = -0.30, CI: -0.49, 0.00,  $pMCMC$  = 0.03; Figure 3;  
114 Table S6). This is consistent with the hypothesis that viviparity is an adaptation to cool  
115 climates (Lambert and Wiens, 2013; Shine, 1985; Watson et al., 2014). However,  
116 reconstructions of ancestral preferred body temperatures of adults indicated that in the  
117 majority of lineages, lower preferred body temperatures evolved after, not before, transitions  
118 to live bearing. This was evident from the lack of difference in  $P_{bt}$  between ancestors of egg-  
119 laying and live-bearing lineages (MR-BPMM, PM = 0.05, CI: -4.47, 2.77,  $pMCMC$  = 0.49;  
120 Table S7).

121 Ancestral reconstructions of  $P_{bt}$  and  $T_{opt}$  of oviparous species showed that transitions  
122 from egg laying to live bearing were not more likely to occur when adult and embryo thermal  
123 optima were similar: 10% of ancestors of live bearing species had aligned embryo and adult  
124 thermal optima compared to 17% of the ancestors of egg laying species ( $\chi^2$  = 0.91, df=1, P=  
125 0.34. Tables S8-S9). As a result, in 90% of egg-laying ancestors of live-bearing species, there  
126 were significant mismatches in thermal optimum with embryos having lower preferred body  
127 temperature compared to adults (Tables S8-S9). There was only one case of  $T_{opt}$  being  
128 significantly higher than  $P_{bt}$  but this was in a lineage with viviparous ancestors and  
129 descendants (Tables S8-S9). In summary, only 10% of the transitions to viviparity are  
130 explained by embryo and adult thermal optima being matched, and the lower  $P_{bt}$  observed for  
131 viviparous taxa appears to have evolved after transitions to live birth, not before.

132

### 133 *Female behavioural plasticity resolves the constraints imposed by thermal physiology*

134 Next, we tested the hypothesis that the thermal mismatch between females and embryos  
135 during the evolution of viviparity is resolved by females adjusting their body temperature  
136 when gravid to meet the thermal requirements of their embryos (Beuchat, 1986). We

137 collected data on the preferred body temperature of gravid ( $P_{bt-g}$ ) and non-gravid ( $P_{bt-ng}$ ) adult  
138 females from 52 species of lizards and snakes from published field and experimental studies  
139 (viviparous  $n = 32$ , oviparous  $n = 20$ . Table S1). Using these data, an effect size of female  
140 behavioural plasticity, Hedges'  $g$  was calculated (positive values = higher  $P_{bt}$  when gravid,  
141 negative values = lower  $P_{bt}$  when gravid).

142         Across the 52 species, there was evidence that females with a high preferred body  
143 temperatures behaviourally reduce their body temperature when gravid more than females  
144 with low preferred body temperatures (Figure 4A; Table S10). This relationship is expected  
145 to be restricted to viviparous lineages if female behavioural plasticity evolves in response to  
146 selection for embryo retention. However, there were comparable negative phylogenetic  
147 correlations between Hedges'  $g$  and  $P_{bt}$  for both oviparous and viviparous taxa, showing that  
148 behavioural adjustment of body temperature when gravid occurs to a similar extent in both  
149 egg-laying and live-bearing species (Egg laying:  $PM = -0.69$ ,  $CI: -0.98, -0.03$ ,  $pMCMC =$   
150  $0.04$ . Live bearing:  $PM = -0.91$ ,  $CI: -0.98, -0.29$ ,  $pMCMC = 0.01$ . Table S11). Furthermore,  
151 ancestral reconstructions of Hedges'  $g$  ('the adjustment of body temperature when gravid')  
152 showed that in lineages with thermal mismatches between adults and embryos, females  
153 adjusted their body temperature when gravid to a much greater extent than where thermal  
154 optima were aligned, in both the ancestors of egg-laying and live-bearing species (MR-  
155 BPMM: Egg-laying ancestors Hedges'  $g$   $PM = -1.07$ ,  $CI = -1.93, -0.59$ ,  $pMCMC < 0.001$ .  
156 Live bearing ancestors Hedges'  $g$   $PM = -1.09$ ,  $CI = -2.73, -0.21$ ,  $pMCMC = 0.004$ . Table  
157 S12). As a result, the inferred Hedges'  $g$  did not differ between the ancestors of oviparous  
158 and viviparous species (Figure 4B), suggesting that behavioural plasticity was present prior to  
159 the emergence of live birth.

160



161 Phylogenetic reconstruction of the transitions in reproductive mode in squamates is a  
162 contentious topic (King and Lee, 2015; Pyron, 2015; Pyron and Burbrink, 2014). Our re-  
163 analysis of published data on reproductive mode recovers similar results to King and Lee  
164 2015 (see methods for information on importance of rate shifts in viviparity), but is not  
165 intended to add to, or resolve, this controversy, which requires greater phylogenetic  
166 resolution and/or data on reproductive mode. For example, the current phylogeny is based on  
167 17 genes and there was substantial variation in the number of estimated origins of viviparity  
168 across the sampled trees ( $n_{\text{species}}$  in tree = 224, median number of origins = 23, range = 12 to  
169 29; see Table S9 for variation in estimated ancestral states across trees). Nevertheless, our  
170 results appear to refute the hypothesis that transitions from oviparity to viviparity have been  
171 limited to lineages where the preferred body temperature of adult females fall within the  
172 thermal tolerance of embryos.

173 Instead, our results suggest that an ancient and evolutionarily conserved ability of  
174 egg-laying females to adjust their body temperature during pregnancy provides a general  
175 resolution to the conflict over adult and embryo thermal optima removing barriers to the  
176 evolution of live bearing. The down-regulation of female body temperature in egg-laying  
177 species while gravid may appear surprising considering that most of these species lay their  
178 eggs within the early stages of development (commonly around the time of limb bud  
179 formation) (Andrews and Mathies, 2000). However, early developmental stages, involving  
180 gastrulation, neurulation and organogenesis, are potentially even more sensitive to  
181 temperature stress than later stages, which are predominantly associated with growth  
182 (Beuchat, 1988b; Sanger et al., 2018). The temperature sensitivity of early-stage embryos  
183 therefore suggests that resolutions to mother-offspring thermal conflicts are required in both  
184 egg-laying and live-bearing species. If true, the key innovation of live birth may owe its

185 evolutionary origin to mechanisms of behavioural temperature regulation put in place long  
186 before live birth emerged.

187         We suggest that the behavioural flexibility of female lizards and snakes enabled the  
188 gradual evolution of live birth by helping traverse potential fitness valleys associated with  
189 embryo retention. In many live-bearing lineages, temperature mismatches have subsequently  
190 been eliminated through the evolution of a lower preferred body temperature in females.  
191 However, extant species demonstrate that behavioural flexibility is frequently maintained in  
192 viviparous lineages that have colonised cool climates. Such behavioural flexibility provides  
193 females with the means to upregulate their thermoregulation in order to maintain embryos at  
194 temperatures significantly warmer than the external environment, and thus contributes to the  
195 adaptive value of viviparity in extant species (Andrews, 2000; Le Henanff et al., 2013; Shine,  
196 1985; Uller and Olsson, 2010; Warner and Shine, 2007). Female thermoregulatory behaviour  
197 therefore appears to be a key adaptation enabling the constraints imposed by thermal  
198 mismatches between mothers and embryos to be overcome. In turn, this has likely facilitated  
199 both the evolution of live birth, and the expansion of reptiles into a variety of environments.

## 200 **Methods**

### 201 *Literature search and data collection*

202 To investigate the relationship between maternal behavioural plasticity and embryo thermal  
203 sensitivity, we used reproductive mode data from Pyron and Burbrink (2014), and collated  
204 existing data to form three datasets: 1) female preferred body temperature ( $P_{bt}$ ) (“ $P_{bt}$   
205 dataset”), 2) the temperature at which hatching success was maximised ( $T_{opt}$ ) (“ $T_{opt}$  dataset”),  
206 and 3) female body temperature when gravid ( $P_{bt-g}$ ) and not gravid ( $P_{bt-ng}$ ) (“Hedges’  $g$   
207 dataset”). Complete data are presented in Table S1. Data were collected for each of the  
208 variables from published literature. We conducted a literature search using ISI *Web of*  
209 *Science* (v.5.30) with search terms specific to each dataset.

210 For ancestral state reconstructions (see details below), we obtained parity mode  
211 (oviparous versus viviparous) data for 8006 squamate species, reconstructed from  
212 phylogenetic analysis (Pyron and Burbrink (2014); Data File 2). We included data only for  
213 species represented in the recent phylogenetic tree used in our main analyses (Tonini et al.,  
214 2016), resulting in a total of 7831 species.

215 The  $P_{bt}$  dataset provided preferred body temperatures ( $P_{bt}$ ) of adult females measured at  
216 one point in time. We used the search terms ‘body temperature\*’, along with one of the  
217 following: ‘squamata\*’, ‘lizard\*’, ‘snake\*’ which yielded a total of 1075 papers. We only  
218 used data from studies where  $P_{bt}$  for females was stated explicitly unless pooled male/female  
219 data stated no significant effect of sex. Data on females that were described to be gravid, or  
220 data collected during the reproductive season were excluded. This provided a final dataset of  
221 female preferred body temperature for 163 species that was independent of the gravid and  
222 non-gravid measures used to calculate Hedges’  $g$  (live bearing:  $n = 61$  and egg laying:  $n =$   
223 103, note  $P_{bt}$  data for *Zootoca vivipara* was available for both reproductive modes and both  
224 were included in the analyses – see below).

225 The  $T_{opt}$  dataset quantified the temperature that maximises embryonic survival (measured  
226 as hatching success;  $T_{opt}$ ) in 51 egg laying species (Figure S1). Hatching success data were  
227 taken from the Reptile Developmental Database (Noble et al., 2018a) and supplemented with  
228 additional studies using the same method described for the  $P_{bt}$  dataset (search terms:  
229 ‘temperature\* AND incubat\* AND hatch\* OR surv\*’, along with one of the following:  
230 ‘squamata\*’, ‘lizard\*’, ‘snake\*’), yielding a total of 671 papers. We only included studies  
231 where three or more constant temperature treatments were used under controlled laboratory  
232 conditions, resulting in 661 papers being rejected due to irrelevance or overlap with the  
233 Reptile Development Database. This resulted in a final  $T_{opt}$  dataset, consisting of 51 species,  
234 obtained from 81 studies.

235

### 236 *Estimating embryo thermal optima ( $T_{opt}$ )*

237 Given that  $T_{opt}$  had a strong phylogenetic signal (Phylogenetic Heritability ( $H^2$ ) = 0.95, 95%  
238 CI: 0.74 – 0.99; Table S4) we fitted a Bayesian Phylogenetic Mixed Effects Model (BPMM)  
239 to hatching success data for all species jointly. Including phylogenetic information allowed  
240 for the  $T_{opt}$  of each species to be estimated with greater accuracy and precision given that the  
241 range and number of temperatures across species varied (range: 10-40 °C, mean number of  
242 temperatures per species  $\pm$  SD:  $7.62 \pm 4.29$ ). Compared to non-phylogenetic models,  $T_{opt}$   
243 estimates produced from phylogenetic models (BPMM) showed smaller sampling error and  
244 avoided convergence problems in estimating model parameters.

245 Importantly, this approach was not used to estimate  $T_{opt}$  data for species without data,  
246 only to better predict  $T_{opt}$  values for species for which there were data. The  $T_{opt}$  BPMM model  
247 was run for 1,100,000 iterations with a burn-in of 100,000 iterations and thinning rate of 500,  
248 leaving us with 2,000 samples from the posterior distribution. Autocorrelation was low (lag  
249 values  $< 0.1$ ) and trace plots showed chains mixed well for all parameters. Our model

250 included temperature as a fixed effect (estimating both a linear and quadratic slopes) and  
251 random slopes of temperature (linear and quadratic slopes) fitted at the phylogenetic level.  
252 From our BPMM we estimated  $T_{opt}$ , and its corresponding sampling variance, using the  
253 posterior distribution of fixed effects and best linear unbiased predictors (BLUPs) for the  
254 random slopes (linear and quadratic) for each species as follows:

$$255 \quad T_{opt} = - \frac{(T_f + T_{sp})}{(2(T_f^2 + T_{sp}^2))}$$

256 Where  $T_f$  and  $T_f^2$  are the posterior linear and quadratic fixed effect estimates for temperature  
257 and  $T_{sp}$  and  $T_{sp}^2$  are the posterior BLUPs for a given species extracted from the phylogenetic  
258 random slopes. Calculating  $T_{opt}$  using the posterior distribution of fixed and random effects  
259 meant that sampling error for a given species could be propagated to subsequent analyses  
260 (see below).

261

### 262 *Estimating Hedges' g*

263 For the final “Hedges' g” dataset, we collected mean, standard deviation and sample sizes for  
264 female preferred body temperatures when gravid ( $P_{bt-g}$ ) and non-gravid ( $P_{bt-ng}$ ) (independent  
265 from the  $P_{bt}$  dataset) from the same study/population. Within the ‘title’, ‘abstract’ or  
266 ‘keywords’ we used search terms ‘body temperature\* AND gravid\* OR reproduct\*’ along  
267 with one of the following: ‘squama\*’, ‘lizard\*’, ‘snake\*’ which yielded a total of 721  
268 papers. An effect size of female adjustment of body temperature when gravid for each species  
269 was measured as the standardised mean differences (Hedges' g) in preferred body  
270 temperatures between non-gravid and gravid females ( $P_{bt-g} - P_{bt-ng}$ ), adjusting for small  
271 sample sizes (Borenstein et al., 2009).

272 We included both field and laboratory measures of female body temperature,  
273 comprising studies that directly compared  $P_{bt-g}$  and  $P_{bt-ng}$ . Only studies that provided both

274 sample size and error around mean of preferred body temperature were included. Of the 721  
275 papers 648 papers were excluded due to irrelevance or insufficient data. Combined, this  
276 yielded a total of 73 studies published up to July 2019 from which effect sizes were  
277 calculated for 52 species (live bearing:  $n = 32$  and egg laying:  $n = 20$ ). Studies used artificial  
278 temperature gradients in the laboratory ( $n = 37$ ) or measured preferred basking temperature in  
279 the field ( $n = 36$ ). Laboratory studies generally measured body temperature in the same  
280 female during gestation ( $P_{bt-g}$ ) and either before or after gestation ( $P_{bt-ng}$ ) as repeated  
281 measures. In contrast, field studies often measured body temperature on a population during  
282 the reproductive season, comparing body temperatures in gravid and non-gravid females at a  
283 single time point. We examined the mean Hedges'  $g$  between laboratory or field studies and  
284 found there were no significant differences (PM (Oviparous) = -0.70, CI = -1.61, 0.60; PM  
285 (Viviparous) = 0.53, CI = -0.25, 1.28. Table S13. See Verification analyses below).

286         The final full dataset (Table S1) contained a total of 224 squamate species. Due to the  
287 inherent paucity of data, particularly for hatching success and body temperature in gravid  
288 females, there was little overlap of species between datasets – we found 39 species had data  
289 available for 2 datasets, while we were only able to obtain data for 4 species across all 3  
290 datasets. Two species in our data are both oviparous and viviparous (*Saiphos equalis* and *Z.*  
291 *vivipara*). For *S. equalis* all data were from an oviparous population, but for *Z. vivipara* there  
292 were data for both oviparous and viviparous populations and we treated these different  
293 reproductive modes as being distinct in our dataset (Recknagel et al., 2018).

294

## 295 **General Statistical Methods**

296 We used Hidden Markov Models (HMMs) to reconstruct ancestral states of viviparity,  
297 Phylogenetic Ridge Regression (PRR) to test for rate shifts in continuous traits across the  
298 phylogenetic tree, and Bayesian Phylogenetic Mixed Effects Models with single (BPMM)

299 and multiple response variables (MR-BPMM) to estimate phylogenetic correlations between  
300 traits and reconstruct ancestral states of continuous variables. All analyses were conducted in  
301 R version 4.0.1(R Core Team, 2020).

302

### 303 *Reconstructing ancestral values of viviparity using Hidden Rate Models (HRM)*

304 The phylogenetic distribution of the evolutionary origins of viviparity in squamates remains  
305 highly debated (Blackburn, 2015a; Pyron, 2015). Our aim here was not to try to resolve this  
306 controversy. However, past literature has highlighted that the rate of evolution of viviparity  
307 varies across squamates, and this has important effects on ancestral reconstructions (Beaulieu  
308 and O’Meara, 2014; King and Lee, 2015; Wright et al., 2015). Not accounting for such rate  
309 variation has resulted in the ancestor of squamates being predicted to be viviparous and many  
310 reversals of viviparity to oviparity, both of which are thought to be unlikely (King and Lee,  
311 2015; Lee and Shine, 2021; Pyron and Burbrink, 2015).

312 We therefore used hidden rate Markov models (HRMs), implemented in the R  
313 package ‘corHMM’ that can estimate variation in the rate of evolution of binary characters  
314 across phylogenies (Beaulieu et al., 2021). To do this, a number of different rate categories  
315 from one state (e.g. oviparity) to another state (e.g. viviparity) are pre-defined and then  
316 estimated across the phylogeny. The most likely number of rate categories can be identified  
317 by comparing AIC values across models with different numbers of pre-defined rate  
318 categories.

319 We found on the trimmed phylogeny (224 species) that AIC values were lowest when  
320 there were 2 rate categories (See R script ‘4. PBT models.R section’). This indicated that in  
321 two clades, transitions to viviparity occurred at a higher rate than in other parts of the  
322 phylogeny (Figure S2). This model produced ancestral estimates that are consistent with the  
323 current predominant view of viviparity evolution across squamates (Blackburn, 2015b; King

324 and Lee, 2015): a root state of oviparity and relatively few reversals of viviparity to oviparity  
325 compared to the transitions from oviparity to viviparity (Table S3).

326 Estimates of ancestral states from HRMs were used to identify transitions between  
327 oviparity and viviparity by classifying nodes in the following way: 1) oviparous with only  
328 oviparous descendants (oviparous to oviparous); 2) viviparous with only viviparous  
329 descendants (viviparous to viviparous); 3) oviparous with at least one viviparous descendant  
330 (oviparous to viviparous); and 4) viviparous with at least one oviparous descendant  
331 (viviparous to oviparous).

332

### 333 *Testing for rate shifts in $T_{opt}$ and $P_{bt}$ using Phylogenetic Ridge Regression (PRR)*

334 We examined whether there was variation in the rates of evolution of  $T_{opt}$  and  $P_{bt}$  across the  
335 trimmed phylogeny (224 species) using phylogenetic ridge regression implemented in the R  
336 package ‘RRphylo’ (Castiglione et al., 2018). We found no evidence that there were rate  
337 shifts in  $T_{opt}$ , but for  $P_{bt}$ , two shifts were identified, one lower and one higher (Figure S2). We  
338 examined how important accounting for such rate variation was for reconstructing ancestral  
339 values of  $P_{bt}$  by comparing estimates from PRR models, both including and excluding clades  
340 with different rates, to estimates gained from BPMMs.

341 We found that ancestral estimates of  $P_{bt}$  from PRR models were correlated to  
342 estimates from BPMMs and this did not change according to whether clades with rates shifts  
343 were included or not (Pearson’s correlation coefficient ( $r$ ): included = 0.72, excluded = 0.72.  
344 See R script ‘4. PBT models.R section’). Given rate shifts had minimal impact on estimates  
345 of ancestral states, we used BPMMs because they: 1) more accurately predicted tip states  
346 than PRRs (BPMMs  $r = 0.84$ , PRRs  $r = 0.60$ ); 2) allow missing data; 3) can incorporate  
347 sampling variances associated with response variables; 4) can be used to calculate  
348 phylogenetic correlations; and 5) can produce distributions of estimates (posterior samples)



349 for each node that enable significant thermal mismatches between embryos and adults to be  
350 estimated (see below).

351

352 *Bayesian Phylogenetic Mixed Effects Models* (BPMM)

353 We implemented BPMMs in *R* with the *MCMCglmm* package (Hadfield, 2010).  $T_{opt}$ ,  $P_{bt}$ ,

354 Hedges'  $g$  were modelled with Gaussian error distributions. The probability of viviparity was

355 modelled using a binary error distribution with a logit link function. For some species there

356 were multiple estimates of Hedges'  $g$ , which was accounted for in two ways. In the main

357 analyses (see specific analyses below for details) where multi-response models were used to

358 examine relationships between traits, a single data point was included for each species.

359 Therefore, a weighted mean for Hedges'  $g$  for each species was calculated. For verification

360 analyses of Hedges'  $g$ , where other traits were not included, species was included as a

361 random effect to account for multiple data points per species.

362 The random effect *animal*, with a covariance matrix derived from the phylogenetic

363 tree was included in all models (Hadfield, 2010). We calculated the phylogenetic signal

364 (equivalent to heritability,  $H^2$ , in the terminology of *MCMCglmm*) for each trait as the

365 variance explained by *animal* relative to total variance (animal and residual). In the case of

366 binary variables (reproductive mode) the residual variance is not identifiable and we

367 therefore used the intraclass coefficient of variation (ICC: phylogenetic variance /

368 (phylogenetic variance + residual variance +  $\pi^{2/3}$ ) \* 100) to examine phylogenetic signature

369 (Nakagawa et al., 2017).

370 Multi-response BPMMs (MR-BPMMs) can also be fitted with *MCMCglmm* that allow

371 the phylogenetic and within-species (residual) correlations between traits to be estimated.

372 Correlations between traits (e.g., A & B) were calculated as:

373

$$\frac{cov(A, B)}{\sqrt{(var(A) \cdot var(B))}}$$

374

375 *Missing data across species*

376 BPMMs permit missing data in response variables which was crucial given the patchy  
377 distribution of the data (Figure 1:  $T_{opt} = 51$  species;  $P_{bt} = 163$  species; Hedges'  $g = 52$   
378 species). The accuracy with which missing data is predicted is related to the phylogenetic  
379 signal in traits and the strength of phylogenetic correlations between traits (Molina-Venegas  
380 et al., 2018). All traits had high phylogenetic signal (phylogenetic heritability  $>70\%$ )  
381 producing high correspondence between raw and predicted values (Figure S2; See also "*The*  
382 *ability of phylogenetic methods to predict missing data in reproductive mode*"). As a result,  
383 our BPMMs enabled us to deal with the fact that not all traits have been measured in all  
384 species.

385

386 *Model convergence, prior settings and characterisation of posterior distributions*

387 Non-informative uniform priors were used for fixed effects and inverse-Wishart priors for  
388 random effects ( $V = 1$ ,  $\nu = 0.002$ ; (Hadfield, 2010)) apart from models with binary response  
389 variables (e.g. reproductive mode). For binary variables the residual variance was fixed to 1  
390 and we specified a fixed effect prior that is relatively flat on the logit scale ( $\mu = 0$ ,  $V =$   
391 residual variance  $\times \pi^{2/3}$ ) and parameter-expanded random effect priors ( $V = 1$ ,  $\nu = 0.002$ ,  
392  $\alpha.\mu = 0$ ,  $\alpha.V = 1000$ ). To examine model convergence we ran three independent  
393 MCMC chains and examined autocorrelation, which was low (lag values  $< 0.1$ ), trace plots,  
394 which showed chains mixed well, and Gelman and Rubin's convergence diagnostic that  
395 models converged (potential scale reduction factors were all below 1.1: R function  
396 `gelman.diag` (Brooks and Gelman, 1998). The convergence of models of the probability of  
397 viviparity (binary response variable) occurred more slowly and therefore were run for longer  
398 (burn-in = 1000000, iterations = 6000000, thinning = 5000). All other models used the run

399 settings specified in the data imputation section. Posterior distributions of all parameters were  
400 characterised using modes and 95% credible intervals (CIs) throughout. Effects were  
401 regarded as significant where CIs did not span 0. *pMCMC* (number of iterations above or  
402 below 0 / total number of iterations) are also presented to facilitate general interpretation.

403

#### 404 *Imputation for missing sampling variances*

405 The accuracy of measures of  $T_{opt}$ ,  $P_{bt}$ , and Hedges'  $g$  varied across species due to study  
406 design and sample sizes which can be accounted for by weighting data points by their inverse  
407 sampling variance using the 'mev' term in *MCMCglmm*. However, missing values in  
408 sampling variances are not permitted in *MCMCglmm*. As data on the error and sample size  
409 was missing for  $T_{opt}$ ,  $P_{bt}$  and Hedges'  $g$  it would not have been possible to account for  
410 sampling error in our analyses without drastically reducing the size of our dataset.

411 Consequently, we used multiple imputation with predictive mean matching in the *mice*  
412 package in R to impute missing error and sample sizes (Buuren and Groothuis-Oudshoorn,  
413 2011). Samples sizes were not available for reproductive mode, but it is typically invariant  
414 within populations leading to minimal measurement error. Therefore, the mev term for  
415 reproductive mode was specified as 0.

416 To incorporate uncertainty in imputations, 20 complete datasets were generated, and  
417 all analyses were conducted by sampling across these datasets. Each model sampled through  
418 the 20 datasets 75 times (1500 sampling events) for 2000 iterations with only the last iteration  
419 being saved. Models that included the probability of viviparity were run for 5000 iterations,  
420 instead of 2000, to reduce autocorrelation amongst posterior samples that is common for  
421 binary variables. Estimates from the last iteration of each sampling event  $i$  were used as the  
422 starting parameter values for the next  $i + 1$ . This led to a posterior sample of 1500 iterations,  
423 the first 500 iterations were discarded as a burn-in and the remaining 1000 (50 per dataset)

424 were used to estimate parameters. Pooling of posterior distributions from model parameters  
425 from across each of the  $n = 20$  datasets enabled imputation uncertainty in sampling variances  
426 to be accounted for.

427

#### 428 *Phylogeny and accounting for phylogenetic uncertainty*

429 We used a recent phylogeny of 9754 squamates (Tonini et al., 2016). For the main analyses  
430 we used 1500 posterior trees to account for phylogenetic uncertainty pruned to the 224  
431 species with thermal data. For BPMMs each model sampled through the 1500 trees using the  
432 same procedure as described for sampling across imputed datasets. Each of the 1500  
433 posterior samples was therefore obtained using a different tree (for similar procedure see  
434 (Ross et al., 2013)). Pooling of posterior distributions from model parameters across trees  
435 allows for phylogenetic uncertainty to be taken into account (Pagel et al., 2004). For  
436 reconstructing ancestral states of viviparity, HRMs were repeated across the 1000 trees used  
437 for estimation in BPMMs. For figures and to examine the sensitivity of ancestral  
438 reconstructions to missing data, we used the maximum clade credibility tree provided by  
439 Tonini et al., (2016).

440

#### 441 *Phylogenetic uncertainty and predicting ancestral states*

442 Quantifying discrepancies between embryo and adult thermal optima in relation to transitions  
443 in reproductive mode requires summarising posterior distributions of estimates of  $T_{opt}$  and  $P_{bt}$   
444 for each node and relating it to its transition category (oviparous to oviparous, viviparous to  
445 viviparous, oviparous to viviparous, viviparous to viviparous). One complication is that for  
446 each node the predicted transition category can vary across trees due to differences in  
447 topology and internal tree structure. Discrepancies between  $T_{opt}$  and  $P_{bt}$  can be estimated for  
448 each transition category for each node, but this becomes problematic when some transition

449 categories for some nodes are rare as it results in few posterior samples to estimate  
450 discrepancies. To circumvent this problem, we estimated the ancestral states for each trait for  
451 each node in each tree (Table S9). Each node was then classified according to the most  
452 frequently predicted transition category and related to posterior distributions of  $T_{opt}$ ,  $P_{bt}$  and  
453 Hedges'  $g$  summarised across all trees.

454

## 455 **Specific Statistical Analyses**

### 456 *Ancestral state reconstructions with missing data*

457 We examined how well models predicted ancestral values of reproductive mode with missing  
458 tip data using HRMs. We first compared the ancestral states of nodes predicted using all  
459 available data on reproductive mode ( $n_{\text{species}} = 7831$ , Table S2) to the predicted states for  
460 same nodes that were obtained using only the trimmed tree and data on species in the thermal  
461 dataset ( $n_{\text{species}} = 224$ , Table S1). Second, we examined the accuracy with which ancestral  
462 nodes could be predicted on the phylogeny of 7831 species using only reproductive mode  
463 data from the 224 species with thermal data. The predicted ancestral states from both these  
464 analyses can be found in Table S3.

465

### 466 *Discrepancies between embryo and adult thermal optima and the evolution of live birth*

467 We conducted six main analyses: **1)** Phylogenetic signature in  $P_{bt}$  and  $T_{opt}$  was estimated  
468 using a MR-BPMM of  $P_{bt}$  and  $T_{opt}$  with heterogenous phylogenetic and residual covariance  
469 matrices fitted as random effects (R code model M1.1. Table S2). **2)** The phylogenetic  
470 correlation between  $P_{bt}$  and  $T_{opt}$  was estimated using a MR-BPMM with unstructured  
471 phylogenetic and residual covariance matrices fitted as random effects (R code model M1.4.  
472 Table S3). **3)** The phylogenetic correlation between the probability of live bearing and  $P_{bt}$   
473 was estimated using a MR-BPMM with unstructured phylogenetic and residual covariance

474 matrices fitted as random effects (R code model M2.1. Table S6). **4)** To quantify the number  
475 of ancestral egg-laying with and without mismatched adult female and embryo thermal  
476 optima a two-step approach was used. The ancestral states of reproductive mode were first  
477 estimated for each node using HRMs (R code model M3\_corHMM). Next a MR-BPPM with  
478  $P_{bt}$ ,  $T_{opt}$  and Hedges'  $g$  as response variables was used (R code model M3.1) to reconstruct  
479 ancestral states for each trait. From this model mismatches in thermal optima (CI of  $P_{bt} - T_{opt}$   
480 not overlapping 0) and levels of female behavioural plasticity were estimated (Table S9 &  
481 S12). **5)** To examine if female plasticity differed between the ancestors of oviparous and  
482 viviparous lineages, with and without mismatched mother-offspring thermal optima, we  
483 examined estimates of Hedges'  $g$  in relation to predicted states of reproductive mode (R code  
484 model M3.1. Table S7 & S12). **6)** The phylogenetic correlation between  $P_{bt}$  and Hedges'  $g$   
485 was estimated across all species (R code model M3.1. Table S10), as well as for egg-laying  
486 and live-bearing species separately using an MR-BPMM with separate unstructured  
487 phylogenetic and residual covariance matrices for each reproductive mode (R code model  
488 M4.1. Table S11).

489

#### 490 *Verification analyses*

#### 491 *Checking for differences in Hedges' $g$ between laboratory and field studies*

492 Differences in the ability of laboratory versus field studies to estimate plasticity in female  
493 body temperature when gravid was examined using a BPMM of Hedges'  $g$  with study type as  
494 a fixed effect (R code model M5.4. Table S13).

495 **Data and code availability**

496 All data and code are publicly available at: <https://doi.org/10.17605/OSF.IO/JT28V>

497

498 **Author Contributions:** Conceptualization, N.F., T.U. and C.K.C; Methodology, D.W.A.N.

499 and C.K.C.; Formal analysis, A.K.P., D.W.A.N. and C.K.C; Investigation, A.K.P.,

500 D.W.A.N., G.M.W. and T.U.; Data curation, A.K.P., D.W.A.N., T.U. and C.K.C; Writing –

501 original draft, A.K.P, N.F., T.U. and C.K.C; Writing – Reviewing & Editing, A.K.P., N.F.,

502 D.W.A.N., G.M.W., T.U and C.K.C; Visualization, A.K.P., D.W.A.N. and C.K.C.;

503 Supervision, T.U. and C.K.C.; Funding acquisition, A.K.P. and T.U.

504

505 **Competing Interest Statement:** The authors declare no competing interests.

506 **References**

- 507 Andrews RM. 2000. Evolution of viviparity in squamate reptiles (*Sceloporus* spp.): a variant  
508 of the cold-climate model. *Journal of Zoology* **250**:243–253. doi:10.1111/j.1469-  
509 7998.2000.tb01075.x
- 510 Andrews RM, Mathies T. 2000. Natural History of Reptilian Development: Constraints on  
511 the Evolution of Viviparity. *BioScience* **50**:227–238. doi:10.1641/0006-  
512 3568(2000)050[0227:NHORDC]2.3.CO;2
- 513 Andrews RM, Mathies T, Warner DA. 2000. Effect of Incubation Temperature on  
514 Morphology, Growth, and Survival of Juvenile *Sceloporus undulatus*. *Herpetological*  
515 *Monographs* **14**:420–431. doi:10.2307/1467055
- 516 Beaulieu J, O’Meara B, Oliver J, Boyko J. 2021. corHMM: Hidden Markov Models of  
517 Character Evolution.
- 518 Beaulieu JM, O’Meara BC. 2014. Hidden Markov Models for Studying the Evolution of  
519 Binary Morphological Characters In: Garamszegi LZ, editor. *Modern Phylogenetic*  
520 *Comparative Methods and Their Application in Evolutionary Biology: Concepts and*  
521 *Practice*. Berlin, Heidelberg: Springer. pp. 395–408. doi:10.1007/978-3-662-43550-  
522 2\_16
- 523 Beuchat CA. 1988a. Temperature effects during gestation in a viviparous lizard. *Journal of*  
524 *Thermal Biology* **13**:135–142. doi:10.1016/0306-4565(88)90024-1
- 525 Beuchat CA. 1988b. Temperature effects during gestation in a viviparous lizard. *Journal of*  
526 *Thermal Biology* **13**:135–142. doi:10.1016/0306-4565(88)90024-1
- 527 Beuchat CA. 1986. Reproductive Influences on the Thermoregulatory Behavior of a Live-  
528 Bearing Lizard. *Copeia* **1986**:971–979. doi:10.2307/1445294
- 529 Blackburn DG. 2015a. Evolution of viviparity in squamate reptiles: Reversibility  
530 reconsidered. *J Exp Zool B Mol Dev Evol* **324**:473–486. doi:10.1002/jez.b.22625



- 531 Blackburn DG. 2015b. Evolution of viviparity in squamate reptiles: Reversibility  
532 reconsidered. *J Exp Zool B Mol Dev Evol* **324**:473–486. doi:10.1002/jez.b.22625
- 533 Blackburn DG. 2006. Squamate Reptiles as Model Organisms for the Evolution of  
534 Viviparity. *Herpetological Monographs* **20**:131–146.
- 535 Borenstein M, Hedges LV, Higgins JP, Rothstein HR. 2009. Effect Sizes Based on  
536 Means Introduction to Meta-Analysis. Chichester, UK: John Wiley & Sons, Ltd. pp.  
537 21–32. doi:10.1002/9780470743386.ch4
- 538 Braña F, Ji X. 2000. Influence of incubation temperature on morphology, locomotor  
539 performance, and early growth of hatchling wall lizards (*Podarcis muralis*). *J Exp*  
540 *Zool* **286**:422–433. doi:10.1002/(sici)1097-010x(20000301)286:4<422::aid-  
541 jez10>3.0.co;2-d
- 542 Brooks SP, Gelman A. 1998. General methods for monitoring convergence of iterative  
543 simulations. *Journal of computational and graphical statistics* **7**:434–455.
- 544 Buuren S van, Groothuis-Oudshoorn K. 2011. mice: Multivariate Imputation by Chained  
545 Equations in R. *Journal of Statistical Software* **45**:1–67. doi:10.18637/jss.v045.i03
- 546 Castiglione S, Tesone G, Piccolo M, Melchionna M, Mondanaro A, Serio C, Di Febbraro M,  
547 Raia P. 2018. A new method for testing evolutionary rate variation and shifts in  
548 phenotypic evolution. *Methods in Ecology and Evolution* **9**:974–983.  
549 doi:10.1111/2041-210X.12954
- 550 Doody JS, Moore JA. 2010. Conceptual model for thermal limits on the distribution of  
551 reptiles. *Herpetological Conservation and Biology* **5**:283–289.
- 552 Du W-G, Shine R, Ma L, Sun B-J. 2019. Adaptive responses of the embryos of birds and  
553 reptiles to spatial and temporal variations in nest temperatures. *Proceedings of the*  
554 *Royal Society B: Biological Sciences* **286**:20192078. doi:10.1098/rspb.2019.2078

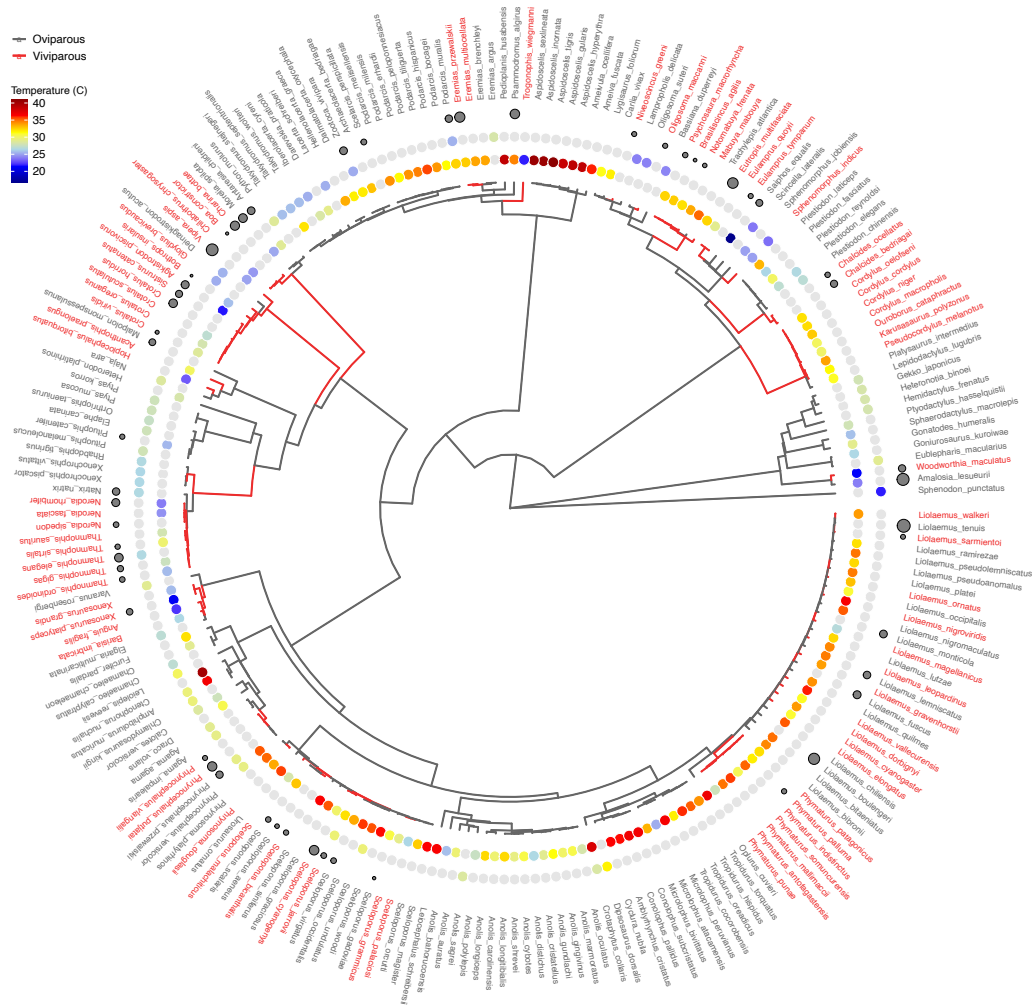
- 555 Hadfield JD. 2010. MCMC Methods for Multi-Response Generalized Linear Mixed Models:  
556 The MCMCglmm R Package. *Journal of Statistical Software* **33**:1–22.  
557 doi:10.18637/jss.v033.i02
- 558 Hadfield JD, Nakagawa S. 2010. General quantitative genetic methods for comparative  
559 biology: phylogenies, taxonomies and multi-trait models for continuous and  
560 categorical characters. *Journal of Evolutionary Biology* **23**:494–508.  
561 doi:10.1111/j.1420-9101.2009.01915.x
- 562 King B, Lee MSY. 2015. Ancestral state reconstruction, rate heterogeneity, and the evolution  
563 of reptile viviparity. *Syst Biol* **64**:532–544. doi:10.1093/sysbio/syv005
- 564 Lambert SM, Wiens JJ. 2013. Evolution of viviparity: a phylogenetic test of the cold-climate  
565 hypothesis in Phrynosomatid lizards. *Evolution* **67**:2614–2630.
- 566 Le Henanff M, Meylan S, Lourdais O. 2013. The sooner the better: reproductive phenology  
567 drives ontogenetic trajectories in a temperate squamate (*Podarcis muralis*). *Biol J Linn  
568 Soc* **108**:384–395. doi:10.1111/j.1095-8312.2012.02005.x
- 569 Lee MSY, Shine R. 2021. Reptilian Viviparity and Dollo’s Law 11.
- 570 Molina-Venegas R, Moreno-Saiz JC, Parga IC, Davies TJ, Peres-Neto PR, Rodríguez MÁ.  
571 2018. Assessing among-lineage variability in phylogenetic imputation of functional  
572 trait datasets. *Ecography* **41**:1740–1749. doi:https://doi.org/10.1111/ecog.03480
- 573 Monasterio C, Shoo LP, Salvador A, Iraeta P, Díaz JA. 2013. High temperature constrains  
574 reproductive success in a temperate lizard: implications for distribution range limits  
575 and the impacts of climate change. *Journal of Zoology* **291**:136–145.  
576 doi:10.1111/jzo.12057
- 577 Nakagawa S. 2015. Missing data: mechanisms, methods, and messages *Ecological Statistics*.  
578 Oxford: Oxford University Press. doi:10.1093/acprof:oso/9780199672547.003.0005

- 579 Nakagawa S, Johnson PCD, Schielzeth H. 2017. The coefficient of determination R<sup>2</sup> and  
580 intra-class correlation coefficient from generalized linear mixed-effects models  
581 revisited and expanded. *Journal of The Royal Society Interface* **14**:20170213.  
582 doi:10.1098/rsif.2017.0213
- 583 Noble DWA, Stenhouse V, Riley JL, Warner DA, While GM, Du W-G, Uller T, Schwanz  
584 LE. 2018a. A comprehensive database of thermal developmental plasticity in reptiles.  
585 *Sci Data* **5**:1–7. doi:10.1038/sdata.2018.138
- 586 Noble DWA, Stenhouse V, Schwanz LE. 2018b. Developmental temperatures and  
587 phenotypic plasticity in reptiles: a systematic review and meta-analysis. *Biological*  
588 *Reviews* **93**:72–97. doi:10.1111/brv.12333
- 589 Pagel M, Meade A, Barker D. 2004. Bayesian Estimation of Ancestral Character States on  
590 Phylogenies. *Systematic Biology* **53**:673–684. doi:10.1080/10635150490522232
- 591 Pyron RA. 2015. Advancing perspectives on parity-mode evolution. *Journal of Experimental*  
592 *Zoology Part B: Molecular and Developmental Evolution* **324**:562–563.  
593 doi:10.1002/jez.b.22644
- 594 Pyron RA, Burbrink FT. 2015. Contrasting models of parity-mode evolution in squamate  
595 reptiles. *Journal of Experimental Zoology Part B: Molecular and Developmental*  
596 *Evolution* **324**:467–472. doi:10.1002/jez.b.22593
- 597 Pyron RA, Burbrink FT. 2014. Early origin of viviparity and multiple reversions to oviparity  
598 in squamate reptiles. *Ecology Letters* **17**:13–21. doi:https://doi.org/10.1111/ele.12168
- 599 R Core Team. 2020. R: A language and environment for statistical computing. R Foundation  
600 for Statistical Computing, Vienna, Austria.
- 601 Recknagel H, Kamenos NA, Elmer KR. 2018. Common lizards break Dollo’s law of  
602 irreversibility: Genome-wide phylogenomics support a single origin of viviparity and

- 603 re-evolution of oviparity. *Molecular Phylogenetics and Evolution* **127**:579–588.  
604 doi:10.1016/j.ympev.2018.05.029
- 605 Ross L, Gardner A, Hardy N, West SA. 2013. Ecology, Not the Genetics of Sex  
606 Determination, Determines Who Helps in Eusocial Populations. *Current Biology*  
607 **23**:2383–2387. doi:10.1016/j.cub.2013.10.013
- 608 Sanger TJ, Kyrkos J, Lachance DJ, Czesny B, Stroud JT. 2018. The effects of thermal stress  
609 on the early development of the lizard *Anolis sagrei*. *Journal of Experimental Zoology*  
610 *Part A: Ecological and Integrative Physiology* **329**:244–251. doi:10.1002/jez.2185
- 611 Shine R. 1995. A new hypothesis for the evolution of viviparity in reptiles. *The American*  
612 *Naturalist* **145**:809–823.
- 613 Shine R. 1985. The evolution of viviparity in reptiles: An ecological analysis *Biology of the*  
614 *Reptilia*, Development B. New York: John Wiley & Sons, Ltd. pp. 605–694.
- 615 Tonini JFR, Beard KH, Ferreira RB, Jetz W, Pyron RA. 2016. Fully-sampled phylogenies of  
616 squamates reveal evolutionary patterns in threat status. *Biological Conservation*,  
617 Advancing reptile conservation: Addressing knowledge gaps and mitigating key  
618 drivers of extinction risk **204**:23–31. doi:10.1016/j.biocon.2016.03.039
- 619 Uller T, Olsson M. 2010. Offspring size and timing of hatching determine survival and  
620 reproductive output in a lizard. *Oecologia* **162**:663–671. doi:10.1007/s00442-009-  
621 1503-x
- 622 Van Damme R, Bauwens D, Braña F, Verheyen RF. 1992. Incubation Temperature  
623 Differentially Affects Hatching Time, Egg Survival, and Hatchling Performance in  
624 the Lizard *Podarcis muralis*. *Herpetologica* **48**:220–228.
- 625 Warner DA, Shine R. 2007. Fitness of juvenile lizards depends on seasonal timing of  
626 hatching, not offspring body size. *Oecologia* **154**:65–73. doi:10.1007/s00442-007-  
627 0809-9

- 628 Watson CM, Makowsky R, Bagley JC. 2014. Reproductive mode evolution in lizards  
629 revisited: updated analyses examining geographic, climatic and phylogenetic effects  
630 support the cold-climate hypothesis. *Journal of Evolutionary Biology* **27**:2767–2780.  
631 doi:10.1111/jeb.12536
- 632 Wright AM, Lyons KM, Brandley MC, Hillis DM. 2015. Which came first: The lizard or the  
633 egg? Robustness in phylogenetic reconstruction of ancestral states. *Journal of*  
634 *Experimental Zoology Part B: Molecular and Developmental Evolution* **324**:504–516.  
635 doi:10.1002/jez.b.22642
- 636

637 **Figures**



638

639 **Figure 1. Variation in reproductive mode, preferred body temperature and plasticity in**

640 **female thermo-regulatory behaviour across 224 species of squamate reptile (lizards and**

641 **snakes). Tips and branches are coloured according to reproductive modes (red = live**

642 **bearing/viviparous, grey = egg laying/oviparous; branch colours represent predicted ancestral**

643 **values; Table S9). Coloured data points correspond to temperature (inner data points**

644 **correspond to the preferred body temperature of female squamates ( $P_{bt}$  dataset, 163 species),**

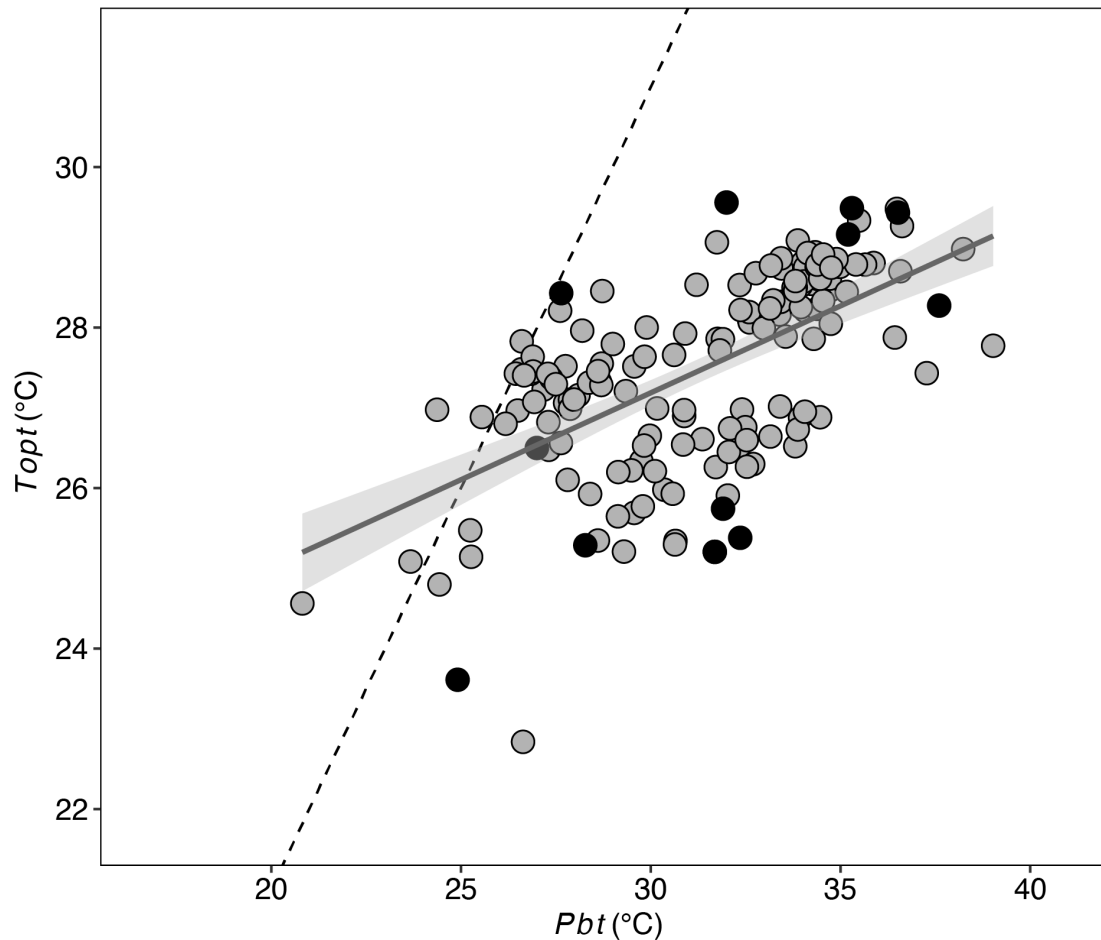
645 **outer data points correspond to the optimal temperature for embryo survival in oviparous**

646 **species ( $T_{opt}$  dataset, 51 species)). The size of the grey data points represent the discrepancy**

647 **between preferred body temperature in gravid versus non-gravid females (Hedges' g dataset;**

648 **absolute values, 52 species).**

649



650

651 **Figure 2. Mismatches in the thermal optima of mothers and embryos across 147**

652 **oviparous species of lizards and snakes.** The relationship between female preferred body

653 temperature ( $P_{bt}$ ) and the temperature that maximizes hatching success of embryos ( $T_{opt}$ )

654 predicted by a multi-response Bayesian Phylogenetic Mixed Model across egg laying species

655 (grey data points, regression lines  $\pm$  95% confidence intervals are plotted). Raw data for 12

656 species with both  $P_{bt}$  and  $T_{opt}$  data shown by black data points. Despite high phylogenetic

657 signature in  $P_{bt}$  and  $T_{opt}$ , there was only weak evidence for co-evolution between the two

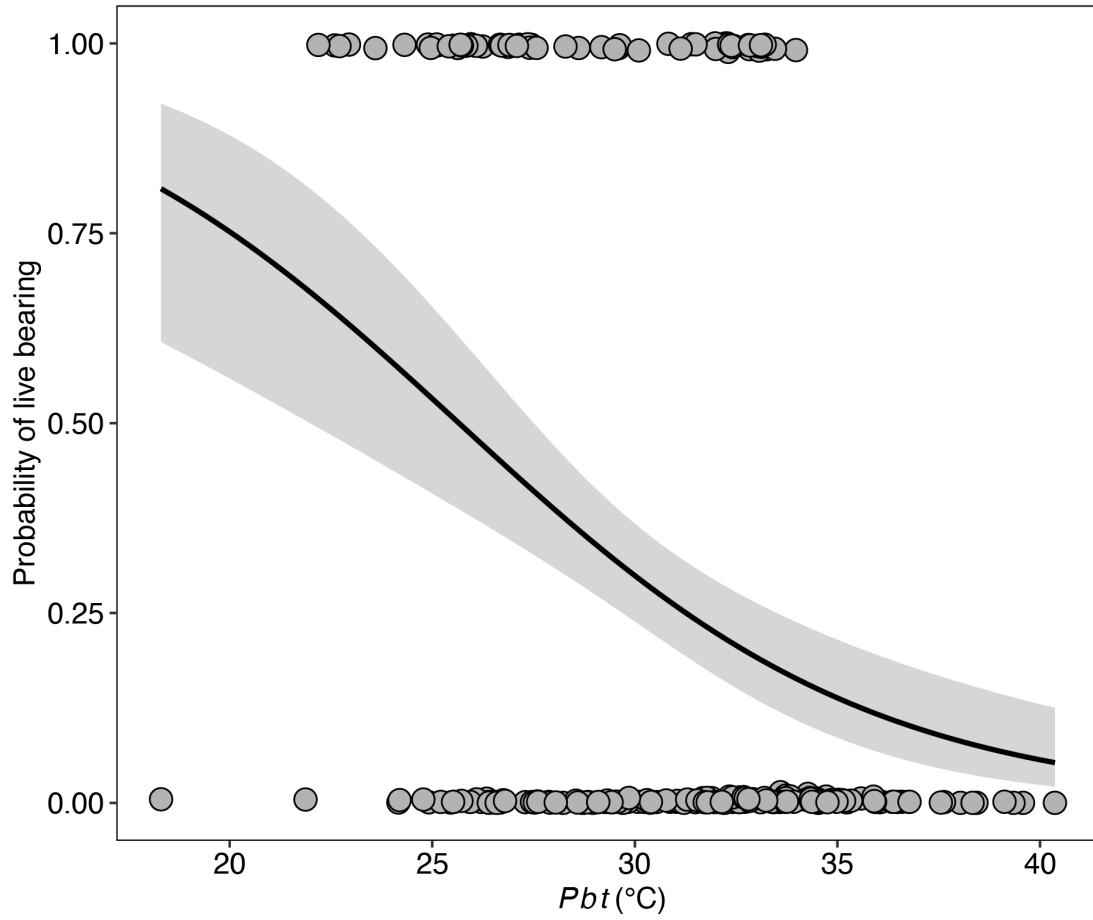
658 traits (Table S5). Deviations from the dotted line (1:1 relationship) indicate the magnitude of

659 the mismatch between adult and embryo thermal optima. Corresponding measurements of

660  $T_{opt}$  and  $P_{bt}$  were not available for all oviparous species (total  $n_{oviparous} = 147$ ,  $n_{P_{bt}} = 103$ ;  $n_{T_{opt}}$

661  $= 47$ ;  $n_{P_{bt}} \& n_{T_{opt}} = 10$ ), hence model predictions rather than raw data are shown (for plot of

662 raw data as well as correspondence between predicted and raw data values see Figure S3).



663

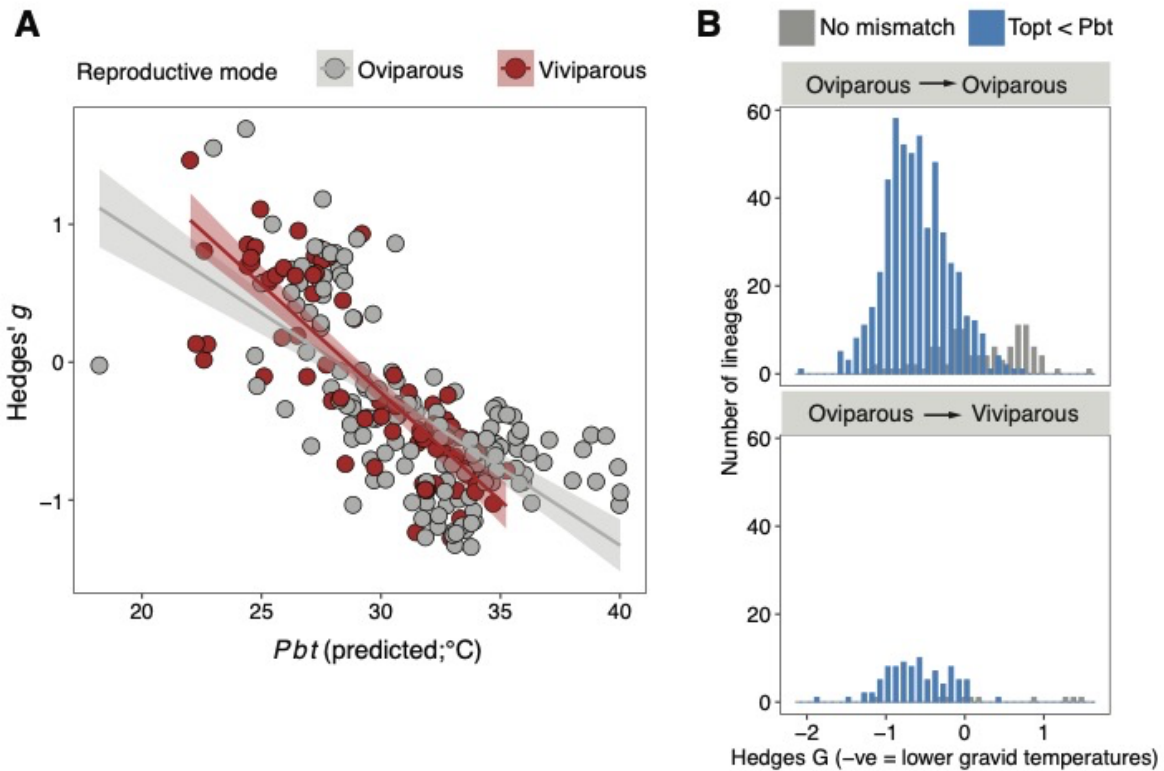
664 **Figure 3. Probability of being a live-bearing species in relation to female non-gravid**

665 **preferred body temperature ( $P_{bt}$ ).** The line and shading represent a logistic regression

666 curve  $\pm$  95% confidence interval.  $P_{bt}$  was obtained for 103 oviparous and 61 viviparous

667 species.





668

669 **Figure 4. Female behavioural plasticity resolves the constraints imposed by thermal**  
670 **physiology, such that transitions to live-bearing (viviparity) occur despite mismatches**  
671 **between females and embryos. (A) Adjustment of body temperature in gravid females in**  
672 **relation to their non-gravid preferred body temperature ( $P_{bt}$ ) across 52 extant oviparous and**  
673 **oviparous lizards and snakes (Hedges'  $g$ ;  $P_{bt-g} - P_{bt-ng}$ ). Regression lines  $\pm$  95% credible**  
674 **intervals are plotted. High values of Hedges'  $g$  signify an increase in body temperature when**  
675 **gravid while low values imply a decrease. (B) The adjustment of body temperature by**  
676 **females in lineages that remained egg laying (top panel) and lineages that evolved live**  
677 **bearing (bottom panel) according to the presence or absence of a thermal mismatch between**  
678 **females and their offspring (inferred from Hedges'  $g$  data shown in panel A).**